Journal of Power Technologies 102 (4) (2022) 175 -- 186

# The Impact of Equivalent Resistance on Power Generation Using PV Module During Different Seasons

Amir Mushtaq, Usman Mussadiq*✉, Anzar Mahmood, Syed Hassan Mujtaba Jafri

Department of Electrical Engineering, Mirpur University of Science and Technology (MUST), Mirpur Azad Jammu and
Kashmir, 10250, Pakistan
✉usman.ee@must.edu.pk

## Abstract

In the promoted study, the impact of equivalent resistance on power generation using pv module during different seasons is calculated as well as measured. The promoter of this research work intends to complete it in different phases: problem identification, data analysis and the description of results. In the first instance, the technical literature has been put into review to bridge the research gap, to estimate the impact of equivalent resistance on power generation by using PV module during changing seasons. In the second step, the impact estimation is made through Simulink model in MATLAB which is previously not used to calculate the power losses to the best of authors knowledge and an experimental study on a 20kW solar-based energy system in the department of Electrical Engineering, Mirpur university of science and technology is also performed. The results find that the series resistance has a direct relation with working temperature and the shunt resistance varies inversely with solar irradiance.

**Keywords**: Solar cells, Equivalent resistance, Distributed energy resources, Green energy

## 1. Introduction

To meet the energy demands of ever-increasing population [1], the fossil fuels-based energy generation is incapable of bridging the demand-supply gap without economic pressure and climatic concerns [2]. The most suitable replacements of traditional resources are solar based energy generation, pneumatic energy, tidal power, geothermal and biofuel [3]. Additional benefits of these replaced energy resources are less cost, the socio-economic [4], the energy access [5] and security [6]. Among these resources, the solar energy can be transformed very easily into electrical energy by using PV cells [7] for building energy management [8], [9]. Presently, the solar energy contribution in world energy mix is 6% and it will gradually go upto 27% till 2050 according to the international energy agency (IEA) [2]. The triplet of PV cells namely monocrystalline, poly crystalline and thin film-based are in use till now which can be connected in both series and parallel combinations to accelerate the voltage and current ratings [10]. They are 1520% efficient and are easily available in the local energy market [11]. The technical advancements are forerunner for the more efficient solar cells [12]. The energy outcome of these cells is highly related to the diversified seasonal parameters namely solar irradiance, site temperature, solar intensity, and time duration. In the focused study, the authors have judged the impact of seasonal dynamics on the output power of the PV module by considering equivalent resistance of a single diode model which is the lacuna filling model, and the comparative technical literature review has been made to the best of authors knowledge. The comparative review

reveals that these modules are mounted on building roof for energy conversion and continual exposure to seasonal dynamics has a considerable effect on module efficiency and system degradation [13]. Further manufacturing defects which are cause of impurities also effect the energy outcomes by altering the module's shunt resistance [14]. Furthermore, the working temperature has a mated relationship with solar irradiance [15] and the study reveals that the solar cell will be 0.41% less efficient with every upcoming degree [16]. In [17], the authors have come to the conclusion that the series resistance is stable to solar irradiance while the shunt resistance drops [18]. The shaded area hinders the light intensity partially or completely and the solar cells start the energy consumption [19]. A dispersed shadow is considered as a source of soft shading while leaves of trees, snow and bird droppings are categorized into the hard source of shading [20].

*Table 1. Nomenclature*

| | | | |
|---|---|---|---|
| STC | Standard testing condition | $K$ | Boltzmann's constant (1.38E–23 J/K) |
| $\eta$ | Diode ideality factor | $T$ | Module temperature (˚C) |
| Eg | Bandgap energy (eV) | $T^*$ | Module temperature at STC (˚C) |
| $G$ | Solar irradiance (W/m2) | $N_s$ | Number of cells in PV module |
| $G^*$ | Solar irradiance at STC (W/m2) | $P$ | Power measured (W) |
| $I_{ph}$ | Photo-generated current (A) | $P_{cal}$ | Power calculated (W) |
| $I$ | Output current of PV module (A) | $Q$ | Electron charge (1.6E–19 Coulomb) |
| $I_{sc}$ | Short circuit current (A) | $R_s$ | Series resistance (Ω) |
| $I_o$ | Reverse leakage current (A) | $R_s^*$ | Series resistance at STC (Ω) |
| $I_o^*$ | Reverse leakage current at STC (A) | $R_{sh}$ | Shunt resistance (Ω) |
| $R_{sh}^*$ | Shunt resistance at STC (Ω) | $V_T$ | Thermal voltage of diode (V) |
| $V$ | Output voltage (V) | $V_{oc}$ | Open circuit voltage (V) |

*Table 2 The relevant studies, research gap and the contributions*

| Reference | Estimation of electrical parameters | | Simulink Modeling | Impact of equivalent Resistance on power generation | Power loss |
|---|---|---|---|---|---|
| | Standard testing condition | Operating condition | | | |
| [10] [13] | X | X | X | ✓ | X |
| [16] [17] | ✓ | ✓ | X | X | X |
| [6] | X | X | X | ✓ | ✓ |
| [26] [27] | ✓ | ✓ | X | ✓ | X |
| Promoted Model | ✓ | ✓ | ✓ | ✓ | ✓ |

In [21], the authors have investigated the impact of dust; mud, talcum or plastic on the power generation using PV cells and the maximum power can be extracted by cleaning the single module with 5-6 liters of water. The transmission losses are also taken as power losses and depend on bundles of photon energy [22]. The photon energy if less than absorption threshold will be insufficient to create electron hole pair while the excessive energy is transformed into heat [23]. In [24], the authors have observed the coated PV modules with

antireflecting film to restrict the power losses caused by reflection. The energy outcomes of PV modules with denatured cells has been calculated in [25].

The authors have estimated the influence of equivalent resistance on PV power generation without calculation of the electrical parameters at the standard testing conditions (STC) and operating conditions (OC) in [10], [13]. However, the afore cited parameters are calculated through STC and OC without estimating the energy outcomes of PV module in [16], [17]. They have calculated electrical parameters at STC and OC without Simulink model along the modules' energy outcomes in [26], [27]. In the promoted model, the calculation of electrical parameters; $I_{ph}$ , $I_o$ , $R_s$ , $R_{sh}$ , $\eta$ and $V_{\mathrm{T}}$ at standard testing conditions (1000 W/m² and 25˚C) and at operating range is carried out numerically as well as experimentally using Simulink and PV analyses respectively. In addition to it, the impact of equivalent resistance on the energy outcomes of PV modules during different seasons is calculated effectively. Table 2 presents relevant literature, research gap and the contributions of the toilsome study. Section II presents the Simulink-based mathematical formulations to estimate the electrical parameters at STC and OC numerically. The experimental study is carried out in Section III. Section IV is dedicated to the results and discussion. The key findings of the research are concluded in Section V.

## 2 Mathematical Formulation

To show the effectiveness of the proposed method for improving power system dynamic stability, a 10- machines 39-bus system is considered for the study. The system is made up of 12 transformers, 34 transmission lines and 19 loads. The total active and reactive loads for the basic configuration are 6145.97 MW and 1363.41 Mvar, respectively. The voltage levels of the test system are 20 kV, 115 kV and 345 kV as shown in Figure **Error! Reference source not found.** with red, blue and black colors, respectively. The numerical investigations were performed using MATLAB/Simulink and all the data used for the system implementation are given in [22].The power losses associated with the equivalent resistance are investigated to estimate the impact of equivalent resistance on power production at different seasons. These losses will be the difference of numerically calculated and the experimentally measured modules' power. In this section, the mathematical formulation is used to calculate the total power using Simulink while in the next section the experimental study is performed for desired results using PV analyzer. The basic characteristic equation of PV cell [28] is given by:

$$I = I_{ph} - I_o\left[\exp\, p^{\left(\frac{\mathrm{V+IR_s}}{\eta \mathrm{N_s V_T}}\right)} - 1\right] + \frac{\mathrm{V + IR_s}}{\mathrm{R_{sh}}} \qquad (1)$$

Where, $I_{ph}$ , $I_o$ and I are denoting the photo generated current, the reverse leakage current and the output current of the PV cell. $V_{\mathrm{T}}$ and $V$ are diode thermal voltage and the output voltage of the PV cell respectively. The number of cells in series or parallel arrangement with resulting resistances are denoted by $N_s$, $R_s$ and $R_{sh}$ respectively. $\eta$ is used for the ideality factor of diode. However, the calculation is carried out without considering the series and shunt resistances and these parameters are supposed to have a 0 weightage in equation 2 for simplification.

$$I = I_{ph} - I_o\left[\exp^{\left(\frac{\mathrm{V}}{\eta N_s \mathrm{V_T}}\right)} - 1\right] \qquad (2)$$

$I_{ph}, I_o, \eta, N_s,$ and $V_{\mathrm{T}}$ are unknown parameters in equation 2. $I_{ph}$ and $I_o$ at operating conditions can be estimated by considering the values of these parameters at standard testing conditions using equations 3-8 [28]. Number of series connected cells (Ns) in PV module are 60 and the output voltage is estimated from the data sheet.

$$\mathrm{I^*_{ph}} = \left[\exp^{\left(\frac{\mathrm{v^*_{mp}} + I^*_{mp}R^*_s}{\eta^* V_T}\right)} - 1\right] I^*_o + \frac{\mathrm{v^*_{mp}} + I^*_{mp}R^*_s}{R^*_{sh}} + I^*_{mp} \qquad (3)$$

$$I_o^* = \frac{\left[\left((R_s^* + R_{sh}^*)I_{sc}^* - V_{oc}^*\right)/(R_{sh}^*)\right]}{\left[\exp^{(V_{oc}^*/\eta V_T)} - \exp^{(Isc_{sc}^* R_s^*/\eta V_T)}\right]} \quad (4)$$

$$R_s^* = \frac{\left[\left(2V_{mp}^* - V_{oc}^*\right)/\left(I_{sc}^* - I_{mp}^*\right)\right]}{\left[\ln(1 - I_{mp}^*/I_{sc}^*)/\left(I_{sc}^* - I_{mp}^*\right)\right]} \quad (5)$$

$$R_{sh}^* = \sqrt{\frac{R_s^*}{(I_{sc}^*/\eta^* V_T)\exp^{(Isc_{sc}^* R_s^* - V_{oc}^*/\eta^* V_T)}}} \quad (6)$$

The value of $R_{sh}^*$, $R_s^*$, $I_o^*$ and $I_{ph}^*$ are used in equation 7 and 8 to calculate the $I_{ph}$ and $I_o$ respectively. The standard testing temperature; $T^*$= 25°C, the solar irradiance at STC; $G^*$=1000 W/m², $E_g{}^*$=$E_g$= 1.1 eV, k = 1.38064852 × 1023 m² kg s$^{-2}$ K$^{-1}$, q=1.60217662×10$^{19}$ C, $V_{mp}$, $V_{Toc}$, $I_{mp}$ and $I_{sc}$ are measured through PV analyzer. $T$ is real time working temperature and measured using temperature sensor while $G$ is measured using solar irradiance meter. Equation 9 and 10 are used to calculate the $V_T$ and $\eta$ respectively.

$$I_{ph} = \frac{G}{G^*}\left[I_{ph}^* + k_i(T - T^*)\right] \quad (7)$$

$$I_o = I_o^*\left(\frac{T}{T^*}\right)^3\left[\exp\frac{1}{k}\left(\frac{E_g^*}{T^*} - \frac{E_g}{T}\right)\right] \quad (8)$$

$$V_T = \frac{kT}{q} \quad (9)$$

$$\eta = \frac{2V_{mp} - V_{oc}}{V_T\left[\ln\left(1 - I_{mp}/I_{sc}\right)I_{mp}/\left(I_{sc}/I_{mp}\right)\right]} \quad (10)$$

By considering all these parameters, the value of I is estimated and used in equation 11 to calculate the modules' power. Finally, the power losses; $P_{Loss}$ is the difference of calculated and the measured values. These losses are due to the equivalent resistances; the series and shunt resistance which are supposed to have no value at the start of calculation process.

$$P_{cal} = VI \quad (11)$$

$$P_{Loss} = P_{cal} - P \quad (12)$$

The Simulink modeling is used for all these calculations to minimize the personal errors and to save the time. The presented model is missing in literature to the best of authors' knowledge. The above equations are used to calculate the unknown parameters which are missing in data sheets [26].

Initially, the values of $R_s$ and $R_{sh}$ are found analytically by using inverse of the slope of V-I curve under short-circuit and open-circuit conditions. Then, the resultant values are used to extract the remaining parameters. Equation 13 and 14 are used to calculate the series and shunt resistances which are not directly measured.

$$R_s = 1 - \frac{P}{P_{cal}} \quad (13)$$

$$R_{sh} = \frac{G}{G^*}R_{sh}^* \quad (14)$$

TableTable 3 presents the calculated values of current ($I$) and power ($P_{cal}$) in three different environmental conditions. It is clear that the calculated current and power during different seasons are low at start of the day and rise gradually at middle and then fall at 7pm.

*Table 3. The calculated values of power and current in different seasons*

| Time | Rainy conditions | | Cloudy conditions | | Sunny conditions | |
|---|---|---|---|---|---|---|
| | (A) | $P_{cal}$ (W) | (A) | $P_{cal}$ (W) | (A) | $P_{cal}$ (W) |
| 08:00 am | 0.55 | 16.4 | 2.92 | 92 | 5.09 | 138 |
| 09:00 am | 0.71 | 21.3 | 3.57 | 111 | 6.09 | 167 |

| | | | | | | |
|---|---|---|---|---|---|---|
| 10:00 am | 0.96 | 29.4 | 3.58 | 107 | 8.5 | 234 |
| 11:00 am | 1.17 | 36.3 | 5.29 | 159 | 8.83 | 229 |
| 12:00 pm | 1.46 | 45.1 | 7.05 | 206 | 9.46 | 262 |
| 01:00 pm | 1.68 | 52.7 | 7.71 | 212 | 9.84 | 253 |
| 02:00 pm | 1.08 | 33.45 | 3.98 | 119 | 9.08 | 237 |
| 03:00 pm | 0.89 | 27.3 | 2.78 | 84 | 7.62 | 204 |
| 04:00 pm | 0.69 | 20.82 | 2.73 | 80 | 4.97 | 135 |
| 05:00 pm | 0.28 | 7.0 | 2.44 | 70 | 2.78 | 78 |
| 06:00 pm | 0.025 | 0.55 | 1.49 | 43 | 1.62 | 45 |
| 07:00 pm | 0.009 | 0.005 | 0.77 | 22.0 | 0.92 | 25 |

*Table 4. Details and specifications of apparatus*

| Apparatus | Model | Specifications | Ratings |
|---|---|---|---|
| PV module | CS6K-275M | Peak power<br>Temperature coefficient<br>Open-circuit voltage<br>Short-circuit current<br>Efficiency<br>Working temperature | W<br>0.053% / ˚C<br>V<br>A<br>16.80%<br>-40˚C 85˚C |
| PV Analyzer | PROVA 210 | Maximum power limit<br>Maximum voltage range<br>Maximum current range<br>Operating temperature | W<br>V<br>A<br>5˚C - 50˚C |
| Solar Irradiance meter | Handyman | Solar Irradiance Range<br>Diode sensor type<br>Hold function<br>Accuracy | to 1999 W/m²<br>Silicon photo diode<br>Hold Min/Max values<br>High accuracy |
| Temperature Sensor | TEK1307 | Temperature range<br>Temperature error margin<br>Sensor type<br>Voltage<br>Working temperature | -50 ˚C 110 ˚C<br>±3 ˚C<br>NTC (10K/3435)<br>1.5V (2xAG13 batteries)<br>0˚C 50 ˚C |

## 3 Experimental Study

In addition to the numerical calculations, the experimental setup is used to measure the current and output power of the PV cell in the department of Electrical Engineering, Mirpur university of science and technology, Mirpur AJK. However, the power loss associated with equivalent resistance neither be calculated nor measured through meters directly. It is estimated by using follows equation 12; the difference of calculated and the measured power. The impact of equivalent resistance is included in the measured value while, it is supposed to be null in the calculation process. Figure Figure 1 enlightens the experimental setup for the presented study. The measurement process is completed by using certain apparatus; the PV analyzer, solar irradiance meter with temperature sensor.

The PV analyzer is connected at the output terminals of PV module, and it is adjusted on auto scan mode. Solar irradiance meter is set to

W/m² range, and the probe of temperature sensor is fixed at the inner side of PV module. Solar irradiance and the temperature are continuous values and during scanning, the average value is selected for the measurement process. The details; the model, with its specifications and ratings of used apparatus namely the PV module, the PV analyzer, solar irradiance meter and the temperature sensor for measurement is presented in Table Table 4. Table Table 5 presents the measured values of current ($I_M$) and power in three different environmental conditions. It is clear that the measured current and power during different seasons are low at start of the day and rise gradually at middle and then fall at night.

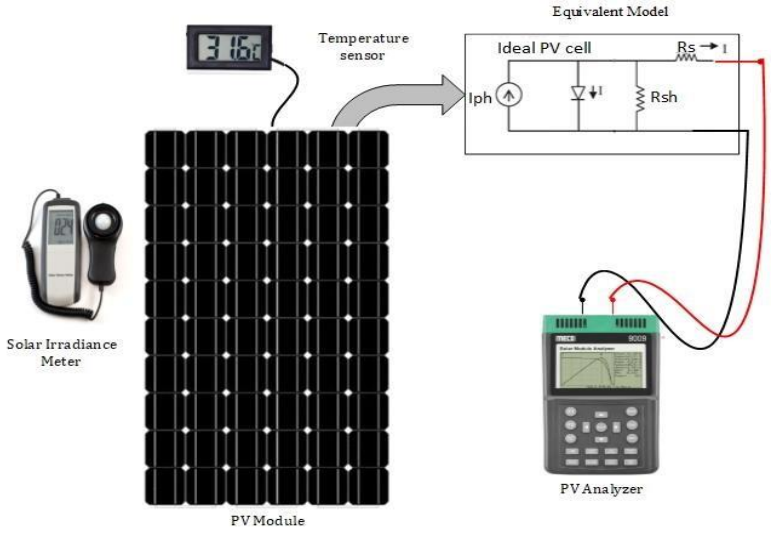


*Figure 1: Experimental setup*

*Table 5. The measured values of power and current in different seasons*

| Time | Rainy conditions | | Cloudy conditions | | Sunny conditions | |
|---|---|---|---|---|---|---|
| | IM (A) | P (W) | IM (A) | P (W) | IM (A) | P (W) |
| 08:00 am | 0.46 | 14.0 | 2.75 | 88.0 | 4.58 | 124.6 |
| 09:00 am | 0.60 | 17.9 | 3.48 | 106.0 | 5.49 | 150.7 |
| 10:00 am | 0.82 | 24.9 | 3.43 | 101.1 | 7.31 | 202.0 |
| 11:00 am | 1.01 | 30.9 | 5.12 | 151.5 | 8.05 | 208.6 |
| 12:00 pm | 1.28 | 39.4 | 6.77 | 196.2 | 8.61 | 241.5 |
| 01:00 pm | 1.49 | 46.8 | 7.02 | 190.0 | 8.93 | 230.1 |
| 02:00 pm | 0.93 | 28.9 | 3.78 | 112.5 | 8.29 | 216.4 |
| 03:00 pm | 0.81 | 24.8 | 2.51 | 76.8 | 6.83 | 186.0 |
| 04:00 pm | 0.59 | 18.0 | 2.45 | 73.7 | 4.37 | 119.0 |
| 05:00 pm | 0.23 | 6.9 | 2.17 | 65.8 | 2.56 | 71.9 |
| 06:00 pm | 0.01 | 0.4 | 1.27 | 39.4 | 1.52 | 42.9 |
| 07:00 pm | 0.005 | 0.003 | 0.60 | 18.0 | 0.85 | 23.6 |

## 4 Results and Discussion

The result clarifies that the shunt resistance of PV cell is solar irradiance dependent. Ideally, shunt resistance is infinite, but it varies inversely with the solar irradiance in practice. It approaches to infinity as irradiance approaches to zero. Figure Figure 2 shows the hourly-based

shunt resistance (kΩ) trend for the average values of solar irradiance (W/m²) in different seasons; rainy, cloudy, and sunny. For instance, in rainy season, the shunt resistance is 210.8 kΩ for the irradiance of 42 W/m² at 08am. While it falls to
61.05 kΩ for the peak value of solar irradiance; 145 W/m² at 1pm. The shunt resistance again rises to the value of 885 kΩ at 7pm, when irradiance reached its minimum value; 0.1 W/m². The similar behavior is observed for the other seasons; cloudy and sunny.

In PV cell, the series resistance is temperature dependent, and it contribute to shape the V-I curve of module. Figure Figure 3 enlightens the direct relation between series resistance and the working temperature in different seasons. The module temperature and the resulting series resistance is constant in rainy season while a sharp trend is observed for these values in cloudy season due to variation of incident photons. Maximum value of series resistance with the temperature peak is observed at 01pm in cloudy season; 0.2056 Ω and 43.5°C respectively. Similarly, the series resistance is considerable throughout the day in sunny conditions because of high temperature of PV module. The incident photons which do not carry photogeneration process and give rise to lattice thermalization because excess energy is transferred into heat are the actual reason behind such high temperature; 60°C at some specified timeslot. These resistances result into the variable current, the power and associated losses regardless of the voltage level.

Figure Figure 4 figures out the impact of the equivalent resistance on the measured current by a competitive trend analysis with the calculated current having zero resistance in different seasons. The calculated current is equal to the measured current, the dissipated current in series resistance and the reverse leakage current, flowing through shunt resistance. In rainy season, when both solar irradiance and module working temperature are low, the output current of PV module is limited to milliamperes. The measured and the calculated currents have a similar value due to negligible equivalent resistance. In addition to it, the difference between these values is slightly higher due to the availability of solar irradiance and working temperature which result into the considerable equivalent resistance.

During summer, the difference between calculated and measured current is remarkable. Figure Figure 5 enlightens the calculated and measured power in different seasons. It clarifies that the calculated power is more than the measured power as the power losses because of equivalent resistances are not considered. The competitive trend also concludes that a considerable power gap exists during the time of high irradiance and working temperature; 10am-03pm in different seasons.

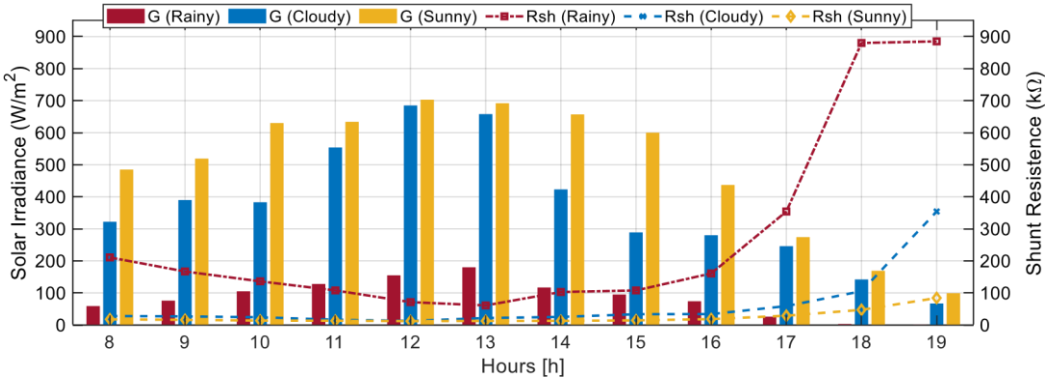


*Figure 2. Solar irradiance and resulting shunt resistance in different seasons*

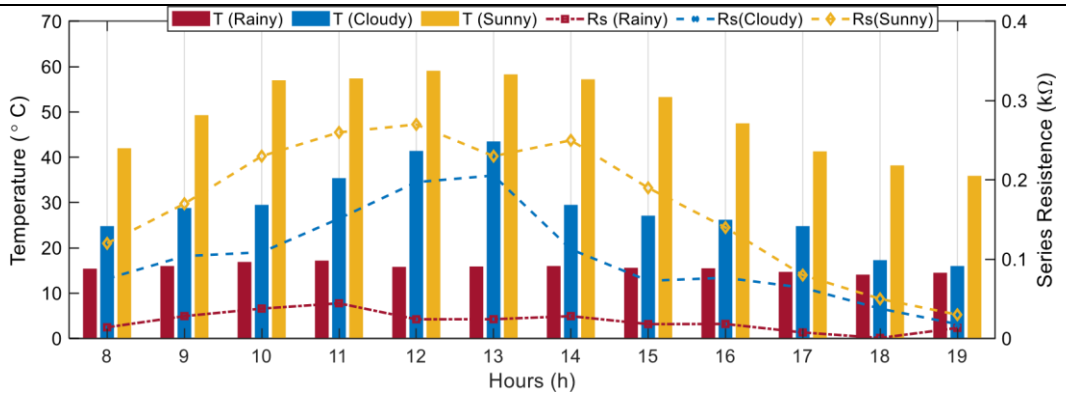


*Figure 3. Temperature and resulting series resistance in different seasons*

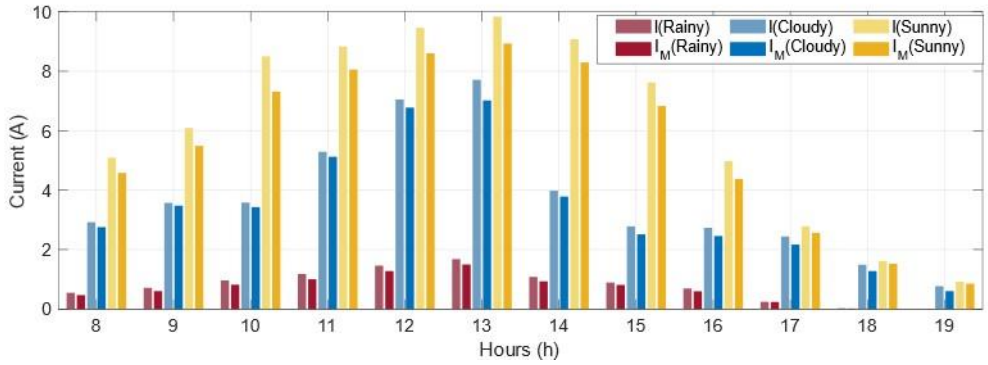


*Figure 4. Measured and calculated current in different seasons*

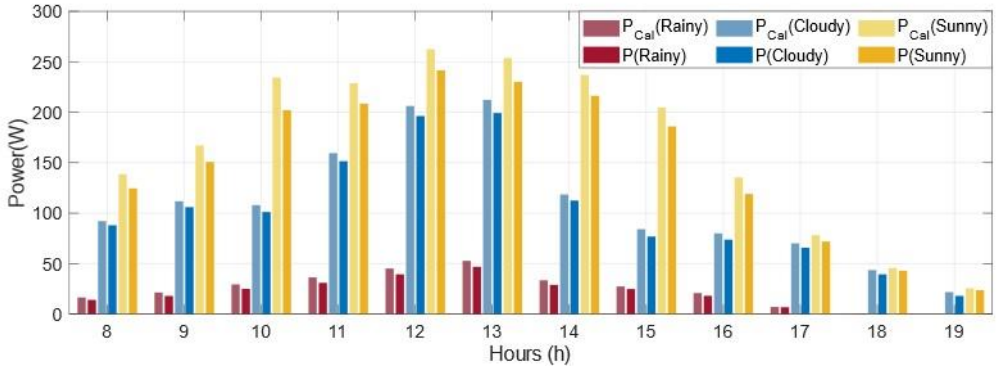


*Figure 5. The measured and calculated power in different seasons*

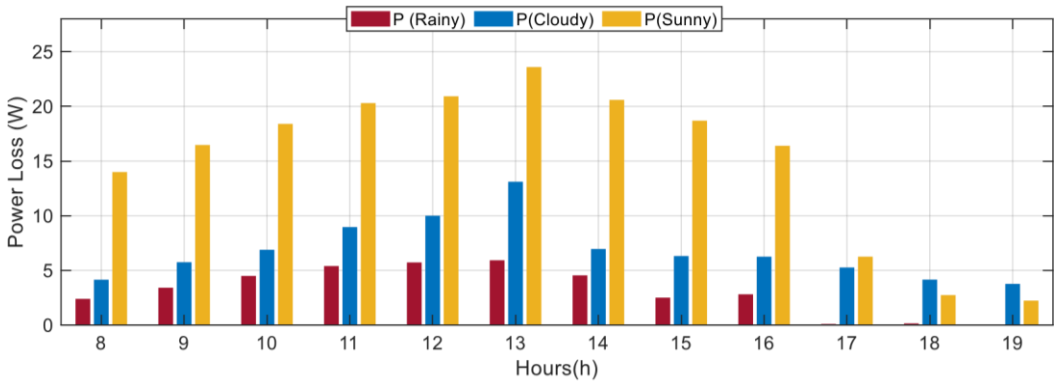


*Figure 6. Power in different seasons*

The irradiance and temperature increase the equivalent resistance of PV module and Figure Figure 6 shows that during the time of high solar intensity and temperature, the power losses in different seasons are considerable. For example, when module temperature does not rise beyond threshold temperature; $25^0$C ± $3^0$C in the presented study, the associated power losses are minimum comparatively the other time slots. Figure 7 shows the interconnection of power losses with series and shunt resistance in different seasons. It is clear from figure that power loss is maximum at low value of shunt resistance and high value of series resistance. In addition to it, the power losses are in direct relation with series resistance and inversely proportional with shunt resistance.

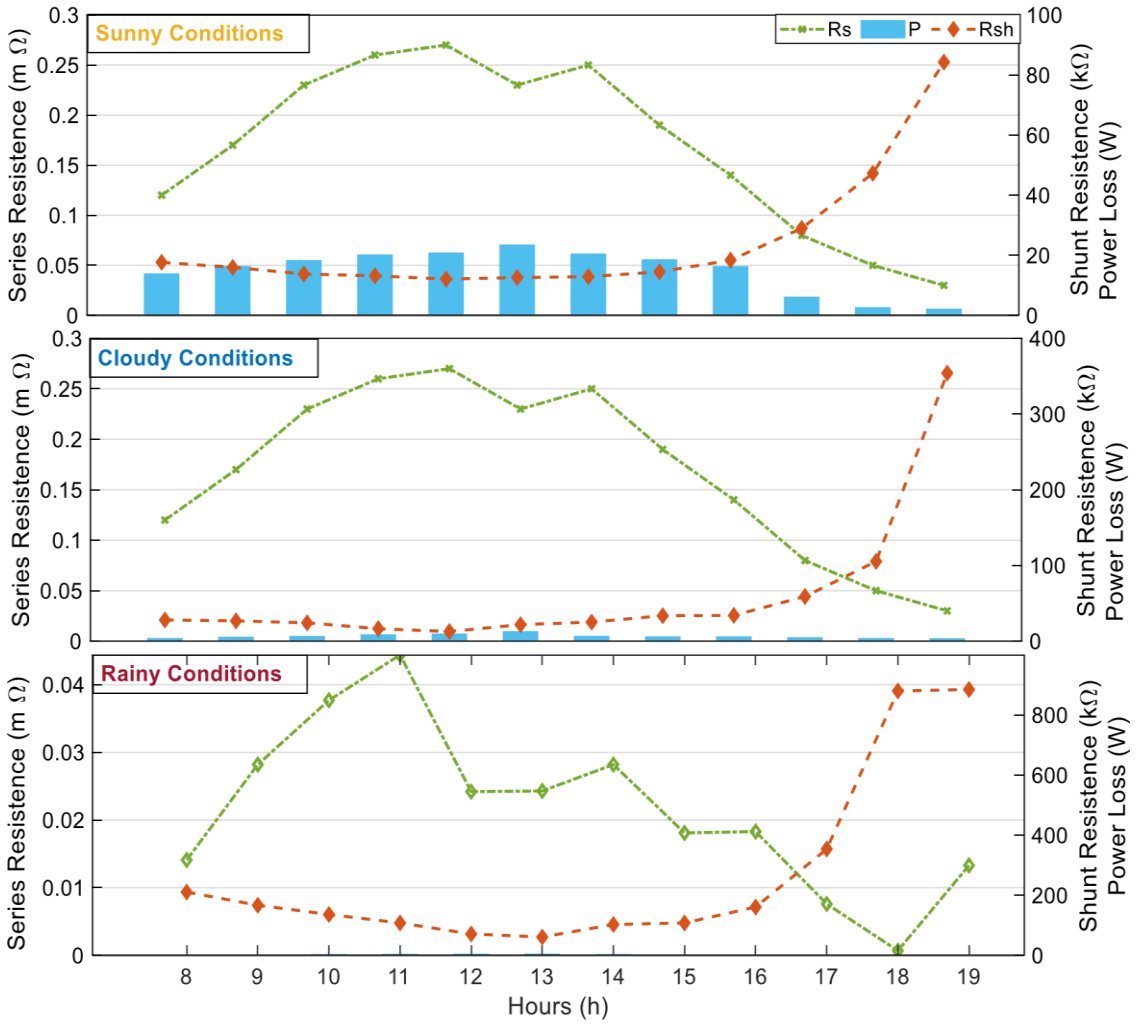


*Figure 7. Power losses trend and the equivalent resistance*

## 5 Conclusion

In the light of the above-mentioned discussion, we have come to the conclusion that there is a very powerful impact of equivalent resistance on PV-based power generation during different seasons. The research work pivots on problem identification, system modeling and description of results. The numerical calculations and experimental study is conducted for the outcome parameters have been given importance. The Simulink modeling is used for numerical statistics while the PV analyzer, irradiance meter and temperature sensors are used for experimental findings. The numerical and experimental studies are integrated to calculate actual yield disturbances. Concluding our talk, we can very confidently say that equivalent resistance has a very powerful impact on power generation during different seasons. This research study will pave the way for the estimation of the aging factor of PV modules. Adding to it, this work can be extended to study the impact of equivalent resistance on other parameters like photocurrent, photovoltage and the diffusion capacity of PV module.

## Acknowledgements

We would like to thank Higher Education Commission for funding grant NRPU#3362 and to extend our cordial gratitude to our colleague Engr. Anila Kousar for providing technical support.

## References

[1] L. Frayssinet, L. Merlier, F. Kuznik, J.L. Hubert, M. Milliez, and J.-J. Roux, "Modeling the heating and cooling energy demand of urban buildings at city scale," *Renewable and Sustainable Energy Reviews,* vol. 81, pp. 23182327, 2018.

[2] C. Tubniyom, R. Chatthaworn, A. Suksri, and T. Wongwuttanasatian, "Minimization of Losses in Solar Photovoltaic Modules by Reconfiguration under Various Patterns of Partial Shading," *Energies,* vol. 12, no. 1, pp. 1-15, 2018.

[3] O. Pupo-Roncallo, J. Campillo, D. Ingham, K. Hughes, and M.Pourkashanian, "Large scale integration of renewable energy sources (RES) in the future Colombian energy system," *Energy,* vol. 186, p. 115805, 2019.

[4] C. Ivanov, "The Challenges Of Achieving Smart, Sustainable And Inclusive Growth In Bulgaria."

[5] A. S. Dagoumas and N. E. Koltsaklis, "Review of models for integrating renewable energy in the generation expansion planning," *Applied Energy,* vol. 242, pp. 1573-1587, 2019.

[6] F. Gökgöz and M. T. Güvercin, "Energy security and renewable energy efficiency in EU," *Renewable and Sustainable Energy Reviews,* vol. 96, pp. 226-239, 2018.

[7] M. B. Hayat, D. Ali, K. C. Monyake, L. Alagha, and N. Ahmed, "Solar energy—A look into power generation, challenges, and a solar-powered future," *International Journal of Energy Research,* vol. 43, no. 3, pp. 1049-1067, 2019.

[8] E. Kabir, P. Kumar, S. Kumar, A. A. Adelodun, and K.-H. Kim, "Solar energy: Potential and future prospects," *Renewable and Sustainable Energy Reviews,* vol. 82, pp. 894-900, 2018.

[9] A. Phayomhom, K. Methapatara, and T. Limlek, "Energy Storage System Application in MEA Building," in *2019 IEEE PES GTD Grand International Conference and Exposition Asia (GTD Asia)*, 2019, pp. 86-91: IEEE.

[10] S. R. Pendem and S. Mikkili, "Modeling, simulation, and performance analysis of PV array configurations (Series, Series-Parallel, Bridge-Linked, and Honey-Comb) to harvest maximum power under various Partial Shading Conditions," *International journal of green energy,* vol. 15, no. 13, pp. 795-812, 2018.

[11] A. Orlandini, "Optimization of PV generator/inverter coupling in terms of DC cable losses and series/parallel connections of PV modules," Politecnico di Torino, 2019.

[12] M. Mathew, N. M. Kumar, and R. P. i Koroth, "Outdoor measurement of mono and poly c-Si PV modules and array characteristics under varying load in hot-humid tropical climate," *Materials Today: Proceedings,* vol. 5, no. 2, pp. 3456-3464, 2018.

[13] A. Omazic *et al.*, "Relation between degradation of polymeric components in crystalline silicon PV module and climatic conditions: A literature review," *Solar Energy Materials and Solar Cells,* vol. 192, pp. 123-133, 2019.

[14] T. D. Lee and A. U. Ebong, "A review of thin film solar cell technologies and challenges," *Renewable and Sustainable Energy Reviews,* vol. 70, pp. 1286-1297, 2017.

[15] S. D. Miller, M. A. Rogers, J. M. Haynes, M. Sengupta, and A. K. Heidinger, "Short-term solar irradiance forecasting via satellite/model coupling," *Solar Energy,* vol. 168, pp. 102-117, 2018.

[16] M. Hammami, S. Torretti, F. Grimaccia, and G. Grandi, "Thermal and performance analysis of a photovoltaic module with an integrated energy storage system," *Applied Sciences,* vol. 7, no. 11, p. 1107, 2017.

[17] M. Chegaar, A. Hamzaoui, A. Namoda, P. Petit, M. Aillerie, and A. Herguth, "Effect of illumination intensity on solar cells parameters," *Energy Procedia,* vol. 36, pp. 722-729, 2013.
[18] C. S. Ruschel, F. P. Gasparin, E. R. Costa, and A. Krenzinger, "Assessment of PV modules shunt resistance dependence on solar irradiance," *Solar Energy,* vol. 133, pp. 35-43, 2016.
[19] B. B. Pannebakker, A. C. de Waal, and W. G. van Sark, "Photovoltaics in the shade: one bypass diode per solar cell revisited," *Progress in photovoltaics: Research and Applications,* vol. 25, no. 10, pp. 836-849, 2017.
[20] M. Hosenuzzaman, N. Rahim, J. Selvaraj, and M. Hasanuzzaman, "Factors affecting the PV based power generation," 2014.
[21] Y. Guan, H. Zhang, B. Xiao, Z. Zhou, and X. Yan, "In-situ investigation of the effect of dust deposition on the performance of polycrystalline silicon photovoltaic modules," *Renewable energy,* vol. 101, pp. 1273-1284, 2017.
[22] L. Shen, Z. Li, and T. Ma, "Analysis of the power loss and quantification of the energy distribution in PV module," *Applied Energy,* vol. 260, p. 114333, 2020.
[23] A. Ivaturi and H. Upadhyaya, "Upconversion and downconversion processes for photovoltaics," in *A Comprehensive Guide to Solar Energy Systems*: Elsevier, 2018, pp. 279-298.
[24] M. R. Maghami, H. Hizam, C. Gomes, M. A. Radzi, M. I. Rezadad, and S. Hajighorbani, "Power loss due to soiling on solar panel: A review," *Renewable and Sustainable Energy Reviews,* vol. 59, pp. 1307-1316, 2016.
[25] F. Spertino, A. Orlandini, and O. G. B. UPC, "Optimization of PV generator/inverter coupling in terms of DC cable losses and series/parallel connections of PV modules," 2019.
[26] R. Sharma, "Parameter extraction for photovoltaic device performance characterization," University of British Columbia, 2017.
[27] H. El Achouby, M. Zaimi, A. Ibral, and E. Assaid, "New analytical approach for modelling effects of temperature and irradiance on physical parameters of photovoltaic solar module," *Energy Conversion and Management,* vol. 177, pp. 258-271, 2018.
[28] R. Abbassi, A. Boudjemline, A. Abbassi, A. Torchani, H. Gasmi, and T. Guesmi, "A numerical-analytical hybrid approach for the identification of SDM solar cell unknown parameters," *Engineering Technology & Applied Science Research,* vol. 8, no. 3, pp. 2907-2913, 2018